JOURNAL OF MATERIALS SCIENCE 29 (1994) 520–526

Molecular deformation processes in gel-spun polyethylene fibres

W. F. WONG, R. J. YOUNG
Polymer Science and Technology Group, Manchester Materials Science Centre, UMIST/University of Manchester, Manchester M60 1QD, UK

The structure/property relationships in the PE fibres have been interpreted quantitatively using a microfibrillar model and the low-strain mechanical properties have been analysed using the Takayanagi models. Information obtained from Raman spectroscopy in the previous paper has been analysed to determine the molecular deformation behaviour of the gel-spun polyethylene (PE) fibres. It is demonstrated that there is a bimodal distribution of stress in the crystalline regions due to the two-phase microstructure of the fibres and it has been shown that the molecular deformation behaviour can be interpreted quantitatively using a parallel-series model. It is found that the Young's modulus of the crystalline regions increases with the degree of chain extension and for the highest-modulus fibres may be close to the theoretical modulus of polyethylene. The fibre modulus is reduced by the presence of low-modulus non-crystalline material in parallel with the crystals.

1. Introduction

Several models have been devised to explain the relationship between the microstructure and mechanical properties of the highly-oriented linear polyethylene (PE) and two very different approaches have generally been used. One approach is the composite model proposed by Barham and Arridge [1, 2] who considered the oriented polymer to consist of a reinforcing needle-like crystal phase embedded in partially-oriented amorphous phase. In this case, the increase in modulus on drawing is postulated as being due to the increase in the aspect ratio of the fibrils and consequently their increased efficiency as reinforcing elements. A completely different model proposed by Peterlin [3, 4] and Gibson *et al.* [5, 6] assumes that the reinforcement comes from taut-tie molecules and inter-crystalline bridges, respectively. They have shown that the increase in modulus with increasing draw ratio could arise primarily from an increase in the proportion of the taut-tie molecules or inter-crystalline bridges rather than from the changing aspect ratio of needle-like crystals [7].

The complete interpretation of mechanical behaviour also requires quantitative models which are capable of relating the mechanical properties to the microstructure of the semicrystalline polymer. There are two distinct types of quantitative models, namely, the aggregate model [7] and the Takayanagi model [8], which have been used to explain the low-strain mechanical behaviour of oriented polymers. However, only the Takayanagi model recognizes the two-phase nature of the semicrystalline polymers and the mechanical behaviour is explained in terms of two separate components representing crystalline and amorphous fractions. This has been used successfully by Gibson *et al.* [5, 6] for the interpretation of the dynamic mechanical properties of the high-modulus PE fibres.

In this study, an attempt has been made to correlate the low-strain mechanical properties of the set of well-characterized high-modulus gel-spun polyethylene fibres described in the previous publication [9] with their microstructure and the results from simultaneous Raman spectroscopy and deformation studies. This enables the molecular behaviour of the gel-spun PE fibres during deformation to be modelled through a combination of the knowledge of the morphology of the fibres with a quantitative analysis of their low-strain mechanical properties. The experimental results are all taken from the previous paper [9] and the same nomenclature, A–I, will be used for the nine fibres studied. All the fibres were gel-spun with the exception of Fibre B which is a melt-spun Snia fibre.

2. Morphological basis of the model

It was shown in the previous publication [9] that by employing a combination of field-emission scanning electron microscopy (FE-SEM) and examination of the replicas of etched surfaces of the monofilaments using transmission electron microscopy (TEM), the morphology of the gel-spun PE fibres is found to be highly crystalline and fibrillar in nature. The fibrils were found to be about 30 nm diameter and of the order of 2–3 μm long [9] and the proposed structural model will therefore be based primarily on the microfibrillar model [3, 4].

Fig. 1 shows a schematic diagram of the proposed structural model that will be employed to explain the observed structure/property relationship of the gel-spun PE fibres [9]. For convenience, the polymer

0022–2461

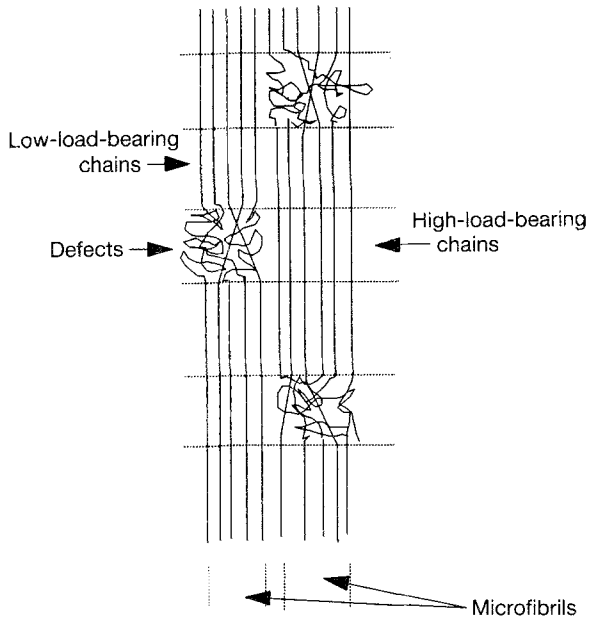

Figure 1 Schematic diagram of the proposed structural model for the gel-spun PE fibres (not to scale).

backbone chains are represented by lines and the crystalline phase is effectively continuous in the direction of the *c*-axis. Within the microfibrils, there are randomly-distributed non-crystalline layers between consecutive, almost fully-oriented crystalline blocks. Although little is known at present about the way in which the linking molecules are arranged in the non-crystalline interface, it is assumed that a fraction of these molecules could be highly chain-extended as for the taut-tie molecules or inter-crystalline bridges proposed by Peterlin [3, 4] and Gibson *et al.* [5, 6], respectively.

At the molecular level, the Raman spectroscopic data show that there is a bimodal stress distribution in the crystalline phase upon deformation [9]. This phenomenon has been confirmed by Moonen *et al.* [10] and Grubb and Li [11] in their Raman spectroscopic work at low temperature. According to these two reports, there are two differently-stressed types of molecular chains within the crystalline phase and this has also been confirmed by wide-angle X-ray diffraction (WAXD) [10]. In our previous study [9], it was found that at around 2% strain, about 40% of the total crystalline material in the structure was in the form of high-load-bearing chains at room temperature. Therefore, the inhomogeneous stress distribution could not be solely due to the presence of a fraction of taut-tie molecules or inter-crystalline bridges in the non-crystalline layers as they are thought to be the minority in the whole highly crystalline fibre structure (with the degree of crystallinity $\phi_c > 85\%$ [9]). Prevorsek has suggested [12] that the bimodal stress distribution during the straining the fibre could be explained as being due to the stress being concentrated on the high-load-bearing chains in the crystalline blocks by the adjacent non-crystalline layer between the two microfibrils as illustrated in Fig. 1. This results in two different populations of stressed molecular chains within the same crystalline phase of the microstructure and this concept is the basis of our present analysis.

3. The Takayanagi model

The Takayanagi model [8] is the simplest way of relating the low-strain mechanical properties of the fibres to the topology of the phases. There are two possible versions of the general model, i.e. parallel-series and series-parallel models and, depending upon the assumptions made about stress transfer between the components, these give different expressions relating the tensile modulus, E, to the microstructure.

3.1. Parallel-series model

In this model, the high-load-bearing crystalline component, C_1, which is induced by the low-modulus defect region of the adjacent microfibril (Fig. 1), is arranged in parallel with the low-load-bearing region which consists of a non-crystalline component A and the low-load-bearing crystalline component, C_2 (Fig. 2). It should be noted that the subscripts 1 and 2 represents the high-load- and low-load-bearing crystal regions, respectively. The non-crystalline component, A, is arranged in series with the second crystalline component, C_2, by assuming there is perfect stress transmission between the two components. However, it is also assumed that there is no stress transmission between the high-load- and low-load-bearing regions. In reality, stress transmission will take place by shear displacement between the components. Unfortunately, this is a fundamental limitation of the Takayanagi model which is unable to take this factor into account.

Previous Raman spectroscopic deformation studies on other high-performance fibres such as aramids [13] have shown that the rate of shift of the Raman peak ($d\Delta\nu/d\varepsilon$) is directly proportional to the tensile modulus, E, i.e.

$$\frac{d\Delta\nu}{d\varepsilon} \propto E = kE \quad (1)$$

where k is a constant. The values of effective modulus for low-load- and high-load-bearing regions can, therefore, be determined from the rates of shift of both narrow and broad Raman peaks respectively measured in the previous study [9].

The quantitative modelling will be carried out using the following assumptions.

1. The volume fractions of the high-load- and low-load-bearing regions are assumed to be proportional to the relative areas, A, of the broad and narrow Raman peaks (fitted to Gaussian curves) [9] i.e. A_1 and A_2, respectively.

2. It is also assumed that there is no Raman scattering from the non-crystalline region.

3. If V_1 and V_2 are the volume fractions of the crystalline components C_1 and C_2, respectively, then together with Assumptions 1 and 2, the relative areas of the two Raman peaks will be equal to the relative volume fractions of each crystalline component.

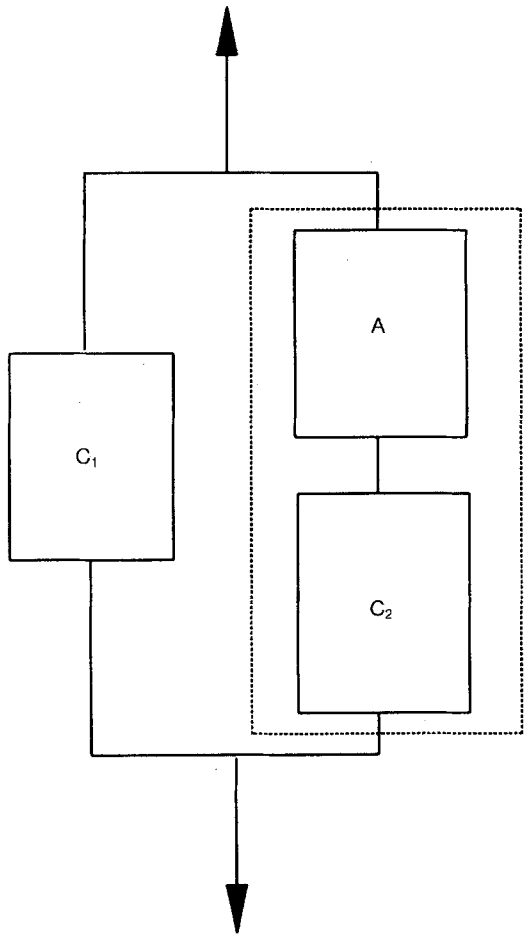

Figure 2 Schematic diagram of the parallel-series Takayanagi model used for gel-spun PE fibres.

Therefore

$$A_1 = \frac{V_1}{V_1 + V_2}$$

$$A_2 = \frac{V_2}{V_1 + V_2} \quad (2)$$

4. Applying tensile stress parallel to the fibre axis will, in general, cause both stretching of the crystallites and a rotation towards the fibres axis due to shear deformation as for aramids [13]. The total strain in the fibre upon straining is usually contributed to by both effects. However, the polyethylene fibres used in this present study all have similar high levels of orientation [9] and so it is assumed that the molecular deformation is dominated by the stretching of the crystallites rather than rotation. Consequently, the change in frequency of the 1128 cm^{-1} C–C symmetric stretching Raman band is a direct measure of the molecular response to straining.

If the volume fraction of the non-crystalline component is V_A, then the fractional degree of crystallinity, ϕ_c, determined from differential scanning calorimetry (DSC) [9] is related to the volume fractions of each component by

$$\phi_c = \frac{V_1 + V_2}{V_1 + V_2 + V_A} \quad (3)$$

The volume fraction of the high-load-bearing region is therefore

$$\frac{V_1}{V_1 + V_2 + V_A} = A_1\phi_c \quad (4)$$

and for the low-load-bearing region is

$$\frac{V_2 + V_A}{V_1 + V_2 + V_A} = 1 - A_1\phi_c \quad (5)$$

Because the high-load-bearing region is in parallel with the low-load-bearing region, the resultant tensile modulus is determined by combining Equations 1, 4 and 5 as

$$E = \frac{1}{k}\left[(A_1\phi_c)\left(\frac{d\Delta\nu}{de}\right)_1 + (1 - A_1\phi_c)\left(\frac{d\Delta\nu}{de}\right)_2\right] \quad (6)$$

where k is the constant in Equation 1 and $(d\Delta\nu/de)_1$ and $(d\Delta\nu/de)_2$ are the rates of shift of the high-load- and low-load-bearing Raman peaks, respectively (Table III in [9]). In Fig. 3, the bracketed term on the right-hand side of Equation 6 is plotted against the experimental modulus, E (corrected for guage length [9]), and it can be seen that the data fall near a straight line with a slope $k = 0.027$ (cm GPa)$^{-1}$ or $(1/k) = 37$ cm GPa. The crystalline components (i.e. C_1 and C_2) in both the high-load- and low-load-bearing regions are assumed to have the same microstructure and they should have the same value of modulus, E_c. Therefore, the modulus of the high-load-bearing region, E_1, can be determined simply through Equation 1 as

$$E_1 = E_c = \frac{1}{k}\left(\frac{d\Delta\nu}{de}\right)_1 \quad (7)$$

From Equation 7, the theoretical rate of shift $(d\Delta\nu/de)_{theo}$ for the 1128 cm^{-1} Raman band is found to be about 8 cm^{-1}/% based on the theoretical crystal modulus for PE of 300 GPa [14]. It is interesting to note that this value is the same order as the value of 14 cm^{-1}/% calculated theoretically by Wool and

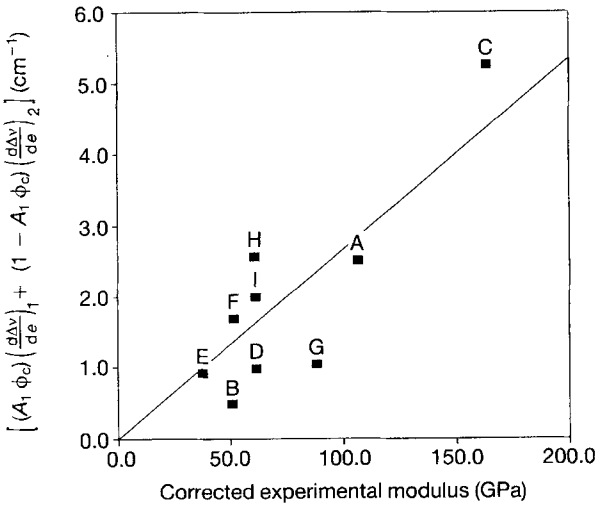

Figure 3 The value of the composite rate of shift of the Raman peaks plotted against the experimentally determined modulus of the fibres (corrected for gauge length) for the parallel-series model.

Bretzlaff [15] based on the anharmonic (Morse) potential energy function for the C–C stretching mode in the PE crystal unit.

In the low-load-bearing region, the non-crystalline component, A, is arranged in series with the crystalline component, C_2, and the effective modulus of the low-load-bearing region, E_2, is given by

$$\frac{1}{E_2} = \frac{1}{E_A}\left(\frac{V_A}{V_2 + V_A}\right) + \frac{1}{E_c}\left(\frac{V_2}{V_2 + V_A}\right)$$
$$= \frac{1}{E_A}\left(1 - \frac{A_2\phi_c}{1 - A_1\phi_c}\right) + \frac{1}{E_c}\left(\frac{A_2\phi_c}{1 - A_1\phi_c}\right) \quad (8)$$

where E_A is the modulus of non-crystalline material in the low-load-bearing region. Therefore

$$E_A = \left(1 - \frac{A_2\phi_c}{1 - A_1\phi_c}\right)\left[\frac{1}{E_2} - \frac{1}{E_c}\left(\frac{A_2\phi_c}{1 - A_1\phi_c}\right)\right]^{-1} \quad (9)$$

Because C_2 is assumed to have the same Young's, E_c, modulus as C_1, then

$$E_2 = \frac{1}{k}\left(\frac{d\Delta\nu}{de}\right)_2 \quad (10)$$

and so E_A can be determined from Equation 9. Fig. 4 shows the dependence of the calculated moduli of both crystalline and non-crystalline components, i.e. E_c and E_A, respectively, upon the experimental fibre modulus. It appears that the highest modulus PE fibre has the value of E_c of $\sim$ 250 GPa which is approaching the theoretical modulus of PE [14]. Interestingly, E_A also increases with the fibre modulus indicating the presence of an increasing number of the taut-tie molecules or inter-crystalline bridges in the non-crystalline phase. Apparently E_c increases at a higher rate than E_A and it appears that even if E_c achieves the theoretical value of 300 GPa, the highest possible experimental modulus that the gel-spun PE fibres can be obtained is $\sim$ 200 GPa using the current technology because of the presence of a lower modulus non-crystalline phase. This relationship between the mechanical properties and the molecular behaviour (from the shift in the frequency of the C–C symmetric stretching mode) shows that the tensile deformation takes place mainly by chain stretching. This is quite different from aramid fibres in which both chain stretching and crystal rotation are thought to be involved during the tensile deformation [13].

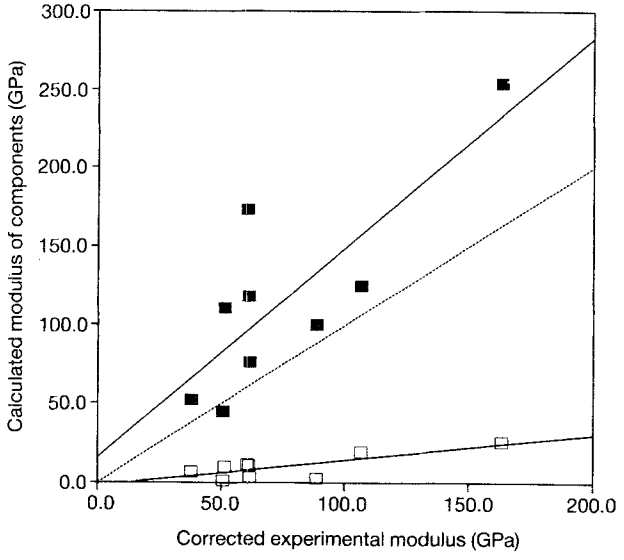

Figure 4 The dependence of the calculated values of (■) crystalline and (□) non-crystalline moduli upon the experimental modulus of the fibres for the parallel-series model. (····) The calculated modulus = fibre modulus.

Another point to note concerns the melt-spun polyethylene fibre, B. It can be seen from Figs 3 and 4 that the data points for this fibre fall on the same line as for the gel-spun fibres, although it has the lowest values of calculated crystal and amorphous modulus. This indicates that as far as the current analysis is concerned, Fibre B behaves in a similar way to the other fibres but with significantly inferior mechanical properties.

3.2. Series-parallel model

It is also important to consider if the behaviour of the fibres could also be analysed using the series-parallel Takayanagi model. The arrangement of this model is illustrated in Fig. 5 with the high-load-bearing crystalline component, C_1, in series with the low-load-bearing region. The low-load-bearing region consists of the crystalline, C_2, and the non-crystalline, A, components arranged in parallel. Based on the same nomenclature used in parallel-series model, the fibre tensile modulus, E, is then related to $(d\Delta\nu/de)_1$ and $(d\Delta\nu/de)_2$ through

$$E = \frac{1}{k}\left\{\left[(A_1\phi_c)\Big/\left(\frac{d\Delta\nu}{de}\right)_1\right] + \left[(1 - A_1\phi_c)\Big/\left(\frac{d\Delta\nu}{de}\right)_2\right]\right\}^{-1} \quad (11)$$

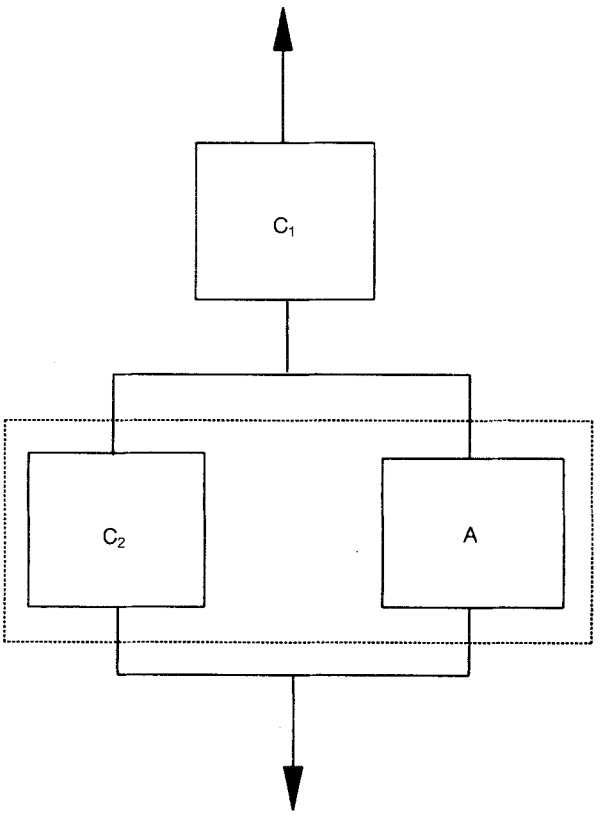

Figure 5 The schematic diagram of the series-parallel Takayanagi model used for the gel-spun PE fibres.

Likewise, a reasonable straight line can be obtained when the bracketed term on the right-hand side of Equation 11 is plotted against the fibre modulus [9] as shown in Fig. 6. The slope of the line gives a slope of $(1/k) = 43$ cm GPa but the agreement is not as good as for the parallel-series model (Fig. 3). It follows that

$$E_1 = E_c = \frac{1}{k}\left(\frac{d\Delta\nu}{de}\right)_1 \quad (12)$$

and the theoretical value of rate of shift $(d\Delta\nu/de)_{theo} = 7\ cm^{-1}/\%$ which is lower than the value of $(d\Delta\nu/de)_{theo}$ for the parallel-series model. Again, the calculated crystalline modulus, E_c, shows a similar relation with the experimental modulus (Fig. 7) as the one obtained by a parallel-series model. For the series-parallel model, the effective modulus of the low-load-bearing region is given by

$$E_2 = E_A\left(\frac{V_A}{V_2 + V_A}\right) + E_c\left(\frac{V_2}{V_2 + V_A}\right) = E_A\left(1 - \frac{A_2\phi_c}{1 - A_1\phi_c}\right) + E_c\left(\frac{A_2\phi_c}{1 - A_1\phi_c}\right) \quad (13)$$

As a result

$$E_A = \left[E_2 - E_c\left(\frac{A_2\phi_c}{1 - A_1\phi_c}\right)\right]\left(1 - \frac{A_2\phi_c}{1 - A_1\phi_c}\right)^{-1} \quad (14)$$

with

$$E_2 = \frac{1}{k}\left(\frac{d\Delta\nu}{de}\right)_2 \quad (15)$$

In this case, all the calculated E_A values are negative as shown in Fig. 8, which demonstrates very clearly that the series-parallel model is not valid for the fibres used in our present study [9]. Clearly, the requirement in the series-parallel model that there is no stress transmission between the crystalline, C_2, and non-crystalline, A, components in the low-load-bearing region is not appropriate nor is the model consistent with the microstructure shown in Fig. 1.

4. High-strain deformation, stress relaxation and creep

Upon straining the fibre, the high-load-bearing region, C_1, is subjected to a high concentration of stress on the molecular chains in the crystalline block adjacent to the non-crystalline layer between the two microfibrils (Fig. 1). Upon further straining, this will result in shear displacement between the microfibrils and consequently an increase in the size of the high-load-bearing region, C_1, as shown in Fig. 9. This is consistent with the finding that the area of the broad high-load-bearing band was found to increase with increasing strain [9]. This concept could also be used to explain the linear relationship between the maximum relative area of the broad Raman peak (high-load-bearing peak) and the corrected strength (Fig. 10) found earlier for the gel-spun fibres [16]. The area of the broad Raman peak is a measure of the number of high-load-bearing chains and it could be assumed to

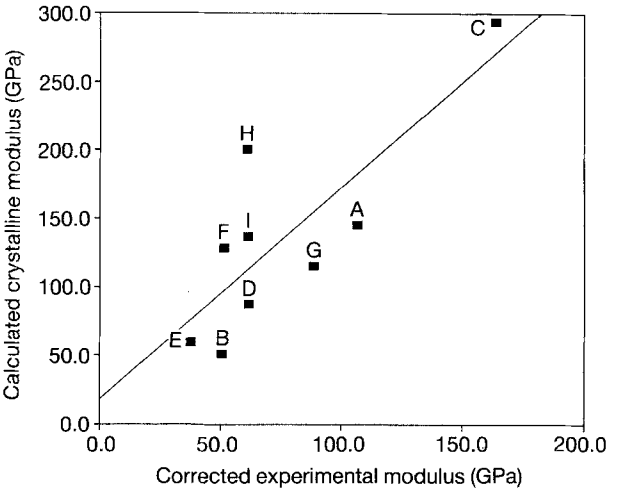

Figure 7 The dependence of the calculated crystalline modulus, E_c, upon the experimental modulus of the fibres for the series-parallel model.

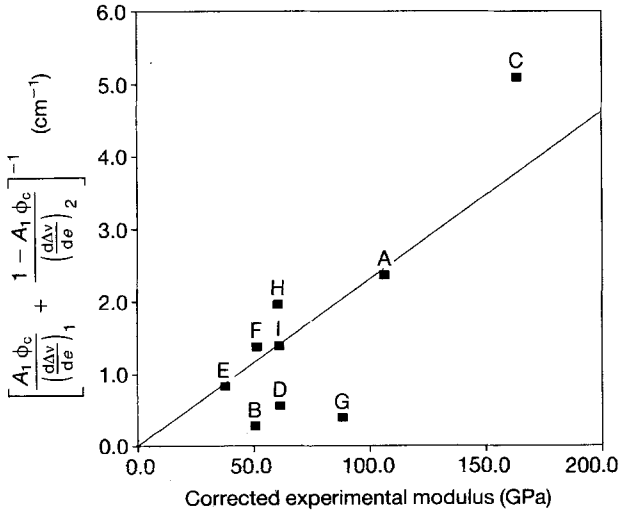

Figure 6 The value of the composite rate of shift of the Raman peaks plotted against the experimental modulus of the fibres for the series-parallel model.

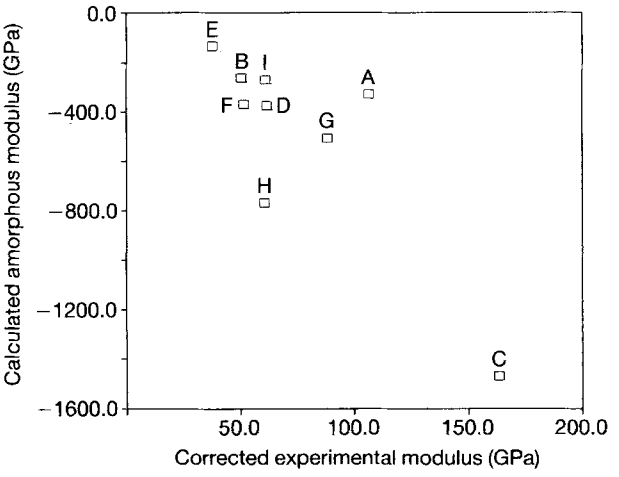

Figure 8 The dependence of the non-crystalline, amorphous modulus, E_A, upon the experimental modulus of the fibres for the series-parallel model.

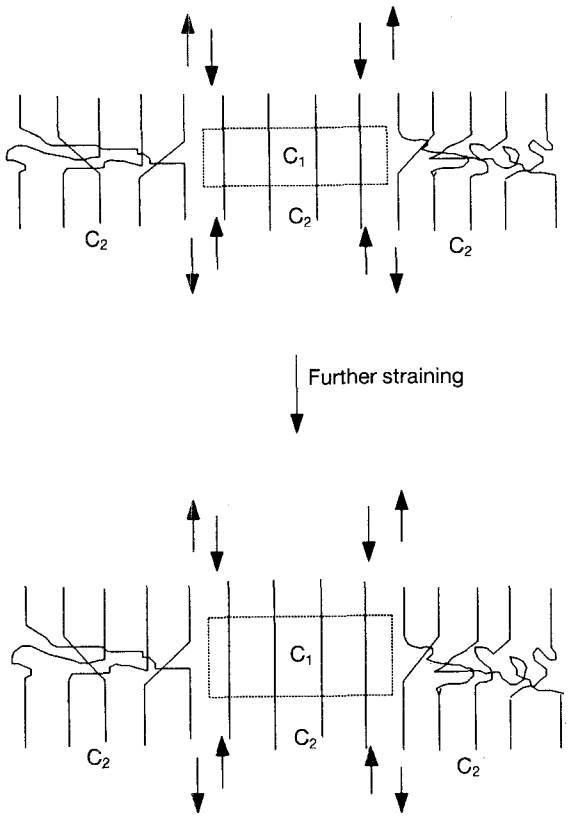

Figure 9 Schematic diagram showing the relative shear displacement of the microfibrils and an increase of the area C_1 of the high-load bearing chains upon straining (not to scale).

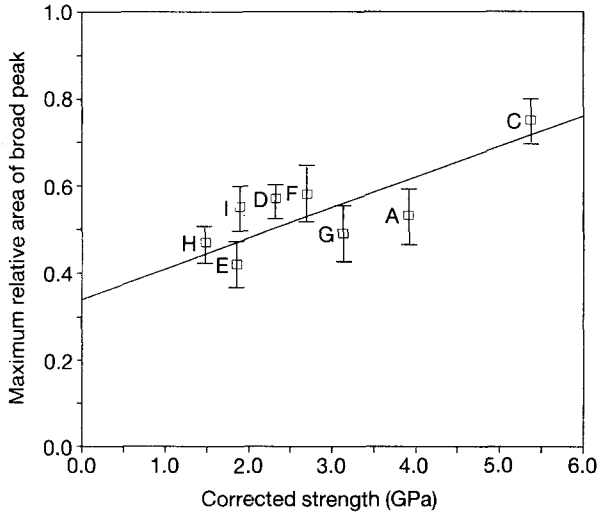

Figure 10 The variation of the maximum relative area of the high-load-bearing Raman peak with fibre strength (corrected for gauge length effects) [9, 16].

be indicative of the volume fraction of region, C_1. However, the maximum in area C_1 was generally attained at a level of strain close to the fibre fracture strain [9]. This shows that at the point of failure the high-load-bearing regions are controlling the fracture strength of the fibres (Fig. 9).

During stress relaxation under constant strain, the wave number of both the low-load- and high-load-bearing peaks were found to shift towards higher wave number [9] indicating the crystalline blocks are becoming subjected to compression. This is probably because on the application of constant displacement, processes such as molecular slippage and molecular disentanglement take place within the non-crystalline regions (Fig. 9). This could result in the non-crystalline region being subjected to higher rate of stress relaxation than the crystalline region which consequently appears to be subjected to a local compressive stress after a period of time. During the creep experiment, a similar positive shift of the Raman bands was observed but it is not as significant as in stress relaxation [9]. Apparently not all the molecular chains within the crystalline region couple efficiently to the applied stress and therefore molecular stress relaxation within the crystalline regions is still possible even though the fibre is under constant applied stress.

5. Conclusions

From the above analysis of structure/property relationships in gel-spun PE fibres [9], it appears that the differences in the mechanical properties of the fibres is due to the difference in properties of individual components in the microstructure. It is, therefore, possible to explain the molecular deformation behaviour observed by Raman microscopy in the high-performance gel-spun PE monofilaments in terms of the microfibrillar model. The low-strain mechanical properties of the fibres can be analysed by the Takayanagi model which can be used to calculate the moduli of both the crystalline and non-crystalline phases in the microstructure. However, sensible results could only be obtained from the parallel-series model which appears to be consistent with the structural model used. Based on this model, it has been shown that both values of crystalline, E_c, and non-crystalline, E_A, modulus increase with increasing values of experimental modulus of the fibres. Apparently the increase of E_c is due to the increasingly higher degree of chain extension in the crystalline phase, while the increase of E_A could be due to the increase of volume fraction of the taut-tie molecules or inter-crystalline bridges. Clearly both factors will be significant in controlling the high-performance mechanical properties of the gel-spun PE fibres.

Acknowledgements

The work was supported by Allied Signal Inc. who also supplied the gel-spun polyethylene fibres. The authors thank Dr D. Prevorsek, Allied Signal, for useful discussion and R.J.Y. is grateful to the Royal Society for support in the form of the Wolfson Research Professorship in Materials Science.

References

1. P. J. BARHAM and R. G. C. ARRIDGE, *J. Polym. Sci. Polym. Phys.* **15** (1977) 1177.
2. R. G. C. ARRIDGE and P. J. BARHAM, *Polymer* **19** (1978) 654.
3. A. PETERLIN, in "Ultra-high Modulus Polymers", edited by A. Ciferri and I. M. Ward (Applied Science, London, 1979) p. 279.

4. A. PETERLIN, in "The Strength and Stiffness of Polymers", edited by A. E. Zachariades and R. S. Porter (Marcel Dekker, New York, 1983) p. 97.
5. A. G. GIBSON, G. R. DAVIES and I. M. WARD, *Polymer* **19** (1978) 683.
6. *Idem, Polym. Eng. Sci.* **20** (1980) 941.
7. I. M. WARD, in "Mechanical Properties of Solid Polymers", 2nd Edn (Wiley, Chichester, 1983).
8. M. TAKAYANAGI, K. IMADA and T. KAJIYAMA, *J. Polym. Sci. C* **15** (1966) 263.
9. W. F. WONG and R. J. YOUNG, *J. Mater. Sci.* **28** (1993) 510.
10. J. A. H. M. MOONEN, W. A. C. ROOVERS, R. J. MEIER and B. J. KIP, *J. Polym. Sci. Polym. Phys.* **30** (1992) 361.
11. D. T. GRUBB and Z. LI, *Polymer* **30** (1992) 2587.
12. D. C. PREVORSEK, Allied-Signal Inc., private communication (1992).
13. R. J. YOUNG, D. LU, R. J. DAY, W. F. KNOFF and H. A. DAVIS, *J. Mater. Sci.* **27** (1992) 5431.
14. L. HOLLIDAY, in "Structure and Properties of Oriented Polymers", edited by I. M. Ward (Applied Science, London, 1975) p. 242.
15. R. P. WOOL and R. S. BRETZLAFF, *J. Polym. Sci.* **B24** (1986) 1039.
16. W. F. WONG, PhD thesis, Victoria University of Manchester (1992).

Received 22 February
and accepted 20 April 1993